A Rapid and Robust Autofocusing Technique for Motion Correction Using Metric Maps

W. Lin[1], H. K. Song[1]

[1]Department of Radiology, University of Pennsylvania, Philadelphia, PA, United States

Introduction: Autofocusing [1-3] has been shown to be an effective post-processing tool for motion correction in MRI. It is an iterative process which involves the application of a series of trial motions to segments of acquired data; the trial position that yields the "best" result, based on a measurement of an image quality metric, is accepted as the actual object position during the acquisition of the data segment. Although shown to achieve results similar to those of navigator echoes in cooperative volunteers [1,2] and for motion along a single axis in clinical data [3], such limited success has not translated to its general applicability in clinical scans. High computational costs and the lack of robustness are the two main drawbacks of existing algorithms. In this work, we propose the use of metric maps, which are plots of the computed image metric values vs. trial translations, for developing improved autofocusing algorithms. A careful study of the metric map properties enables several significant improvements to the optimization process. The effectiveness of the improved algorithm is demonstrated for in-plane translational motion in phantom and in vivo high-resolution MR images.

Theory: The effect of motion on image quality could be simulated by applying a series of trial motions to a portion of k-space (*S*), while the remainder (*B*) used for the analysis remains motionless (**Fig. 1a**). After zero-filling to the full resolution, the data is Fourier transformed to image space, and an image metric computed. Normalized gradient squared (NGS) [4] was used in this work, although other metrics such as entropy could also be used. Metric maps for the various sizes and locations of *S* are shown in **Fig. 1b**. For these map, *B* only includes the k_y lines more central than *S*. This choice of *B* is essential since if one chooses a center-out approach, in which motion compensation proceeds starting from the central k-space region [2], the assumption that data in *B* be motion-free would always be valid. The metric maps are characterized by a consistent pattern, in which there is a narrow band along the phase-encoding (y) direction, oscillating at a frequency corresponding to the average spatial frequency of segment *S*. If *S* contains only one line (n=1), the oscillations are perfectly periodic due to the wrap in phase. With more lines, however, there is a global maximum at the center of the maps ($\delta x, \delta y$)=(0,0) corresponding to the motion-free state. In the presence of translational motion, the metric map will be shifted along the x- and y-directions, and the goal of a successful autofocusing algorithm is to locate the maximum. Metric maps consistently show the described patterns for various image metrics including entropy, as well as for different imaging objects examined in this study.

Methods: Based on the observed patterns, a global optimization strategy was devised that first locates the x-axis shift of the oscillating band followed by a successive 1-D search to find the global maximum. In the first step, the range of search includes the full trial motion range along x, but is limited to one oscillation cycle along y. A step size of 1 pixel along x and one-fourth of the oscillation period along y are sufficient to locate the oscillating band. In the second step, starting from the maximum detected from the first step, 1-D searches in the two directions are alternated until the location of the maximum no longer changes. The final search step size was 1/4 pixel in both directions. As mentioned above, the strategy proceeds outward starting from the central k-space. The proposed algorithm was compared with previous autofocusing techniques in a phantom experiment with manually applied translations. The algorithm was also applied to motion-corrupted in vivo high-resolution MR images of trabecular bone in the distal radius of three subjects, and the results compared with those corrected using 2D navigator echoes [5]. The in vivo parameters include: 3D FLASE pulse sequence, 137x137x500μm^3 voxel size, 512x256x32 matrix, TR/TE=80/7.8 ms, and SNR~9. The 3D data were first Fourier transformed to separate the slices (inner-most acquisition loop), and a 2D correction applied on a single slice.

Results and Discussion: Phantom experiment results shown in **Fig. 2** demonstrate that the proposed optimization scheme is superior to previous methods. For in vivo high-resolution MR images, the improved algorithm yields metric values higher (by an average of 16%) than those obtained with navigator correction. Results from one of the subjects are shown in **Fig. 3**. The motion trajectories recovered closely parallels those recovered by navigator data (**Fig. 4**), containing both smooth continuous motion as well as several sudden jumps. The increased errors in Δy at the edges of k-space do not affect the image quality significantly due to the wrap in the phase [1]. The processing times averaged approximately 2 minutes in these experiments, a speed gain of about an order of magnitude compared to full search methods. The computation time is similar to that of previous 1-D successive techniques, but the results demonstrate significant improvements using the proposed scheme. The in vivo experiments also demonstrate that the proposed autofocusing scheme could be used in clinical images with limited SNR (~9).

Conclusion: An improved autofocusing algorithm is proposed exploiting the patterns observed in image quality metric maps. The algorithm is fast and is more robust than existing methods. Successful motion compensation has been demonstrated in both phantom studies and in vivo examinations.

Acknowledgements: NSF BES-0302251

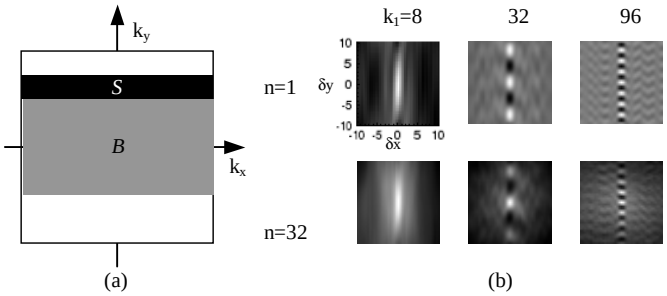

Fig. 1 (a) The k-space region used for the metric map consists of segment *S*, to which the trial motions are applied, and the motion-free "background" *B*, which may contain only a portion of the remaining data. (b) Metric maps (NGS) computed from a 256x256 head image, for segment *S* that contains k_y lines in the range $[k_1,k_1+n-1]$, where $k_y=0$ is the k-space center. Maximum metric value corresponds to the best image quality. Applied translations ($\delta x,\delta y$) are in pixels.

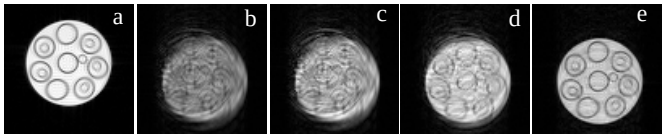

Fig. 2 Comparison of different autofocusing schemes in a phantom experiment. (a) Motion-free control; (b) Motion-corrupted; (c)–(e) Autofocused images: (c) Original technique [1] (d) 1-D successive optimization [2]; and (e) Proposed technique.

References:

[1] Atkinson D, et al., *IEEE Tran. Med. Imag.* 1997; 16(6):903-910

[2] Atkinson D, et al., *Magn. Reson. Med.* 1999; 41:163-170.

[3] Manduca A, et al., *Radiology*. 2000; 215:904-909

[4] McGee KP, et al., *J. Magn. Reson. Imag*. 2000; 11: 174-181.

[5] Song HK, et al., *Magn. Reson. Med.* 1999; 41:947-953.

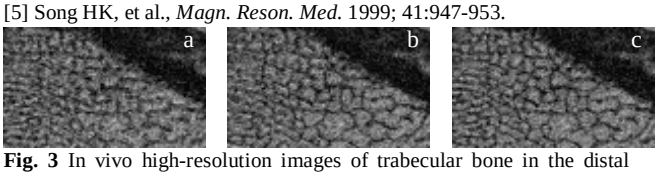

Fig. 3 In vivo high-resolution images of trabecular bone in the distal radius cropped to show details. (a) Motion-corrupted; (b) Navigator-corrected; and (c) Autofocused with the proposed algorithm.

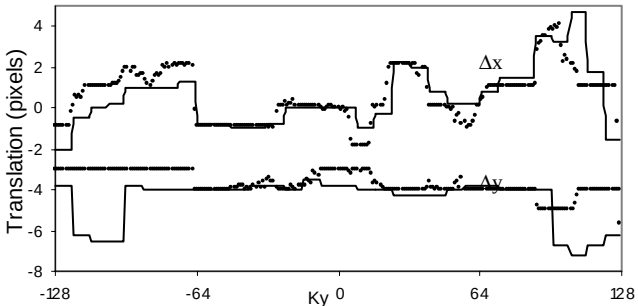

Fig. 4 Comparison of motion recovered with the proposed technique (lines) and with navigators (dots) for images shown in **Fig. 3**.